

A Practical Guide to the Partition Function of Atoms and Ions

P. ALIMOHAMADI¹ AND G. J. FERLAND¹

¹*University of Kentucky, Lexington, KY 40506, USA*

ABSTRACT

The partition function, U , the number of available states in an atom or molecules, is crucial for understanding the physical state of any astrophysical system in thermodynamic equilibrium. There are surprisingly few *useful* discussions of the partition function's numerical value. Textbooks often define U ; some give tables of representative values, while others do a deep dive into the theory of a dense plasma. Most say that it depends on temperature, atomic structure, density, and that it diverges, that is, it goes to infinity, at high temperatures, but few give practical examples. We aim to rectify this. We show that there are two limits, 1 & 2 electron (or closed-shell) systems like H or He, and species with a complicated electronic structure like C, N, O, and Fe. The high-temperature divergence does not occur for 1 & 2 electron systems in practical situations since, at high temperatures, species are collisionally ionized to higher ionization stages and are not abundant. The partition function is then close to the statistical weight of the ground state. There is no such simplification for many-electron species. U is temperature-sensitive across the range of temperatures where an ion is abundant but remains finite at even the highest practical temperatures. The actual value depends on highly uncertain truncation theories in high-density plasmas. We show that there are various theories for continuum lowering but that they are not in good agreement. This remains a long-standing unsolved problem.

Keywords: partition function - dense plasma - hydrogen - many-electron

Contents

| | |
|--|----|
| 1. Introduction | 1 |
| 2. The partition function in astrophysics | 2 |
| 2.1. Notation in this tutorial | 2 |
| 2.2. Range of density and temperature | 2 |
| 2.3. Definition of the partition function | 3 |
| 2.4. Ionization and excitation - the Boltzmann and Saha equations | 3 |
| 2.5. The partition function for an infinite and finite atom | 5 |
| 2.5.1. The divergent partition function for an infinite level atom | 5 |
| 2.5.2. The partition function for a finite atom | 6 |
| 3. The truncation of the partition function | 8 |
| 3.1. Inter-particle interactions with Sharp cut-off | 8 |
| 3.2. Inter-particle interactions with smooth cut-off | 10 |
| 4. One and two-electron systems; a simple limit | 12 |
| 4.1. Asymptotic model with the Saha equation | 12 |
| 4.2. A practical upper limit to the temperature | 14 |
| 5. Complex ions - here be dragons | 16 |
| 6. The molecular partition function | 21 |
| 7. Discussion, summary, and conclusion | 21 |
| References | 23 |

1. INTRODUCTION

The partition function U is the number of available states of an atom or molecules. It is at the heart of computing the Local Thermodynamic Equilibrium (LTE) level occupation of atoms and ions using the Boltzmann equation and the ionization of each chemical element using the Saha equation. Calculating its numerical values is not a simple task because of the well-known divergence at high temperatures, which is discussed below. Also, despite its critical importance, we know of no general introduction to the numerical value of the U for atoms and ions (we do not consider molecules here). This tutorial aims to this.

Here, we provide a brief survey of discussions of the partition function in astrophysical textbooks. [Carroll & Ostlie \(2006\)](#) gives an equation for the partition function, but with no more detail. [Blundell & Blundell \(2010\)](#) defines the partition function as the sum over the Boltzmann factor without considering the degeneracy of each level determined by the statistical weight. This is a hypothetical two-level system introduced only for tutorial purposes. [Bradt \(2014\)](#) lists the partition function as just due to the ground state. At the opposite extreme, [Hubeny & Mihalas \(2014\)](#) gives an extensive summary of the theory described by [Hummer & Mihalas \(1988\)](#), but it provides no numerical values, while [Griem \(2005\)](#) presents an even more formal discussion from the laboratory plasma perspective. Some books ([Swihart 1968](#); [Novotny 1973](#); [Allen 1973](#); [Cox 2000](#)) give tables of values for selected species over specific temperatures, but there is no detail of the procedures used nor guidance for the density or temperature dependence. [Novotny \(1973\)](#) and [Swihart \(1968\)](#), give U and comment that the reported values are valid regardless of temperature if the ion is abundant. [de Galan et al. \(1968\)](#); [Sauval & Tatum \(1984\)](#) give polynomial expressions for the partition function versus temperature, which give approximate estimates of U , but do not describe the density dependence.

our goal is to discuss the densities and temperature dependencies of atomic and ionic partition functions. We begin by considering the simplest and most important case, atomic hydrogen. We demonstrate its divergence over a very larger temperature range and demonstrate its divergence. We give an overview of some theories for how to treat the very high states that cause the function to diverge. The Saha equation shows that atomic hydrogen will not be abundant when the tem-

perature is high enough for U to diverge. This simplifies the partition function for most densities and temperatures since it becomes the statistical weight of the ground state. We then go on to consider many-electron systems with their complex energy structure. A robust and reliable theory of continuum-lowering and dense-plasma effects is needed to handle finite densities properly. These effects limit the number of states that contribute to U and prevent its divergence. There are different physical theories, used in different communities, which do not agree well.

2. THE PARTITION FUNCTION IN ASTROPHYSICS

2.1. *Notation in this tutorial*

The current convention in astrophysics is to express column density as N [cm^{-2}] and the particle number-density as n [cm^{-3}]. Here we use n for the principal quantum number and N for the number-density.

There are different notations, such as Q , Z , and U for the partition function. We use U for the partition function.

2.2. *Range of density and temperature*

We discuss temperatures ranging between 2.7 K and 10^8 K. The temperature $T = 2.7$ K is the lowest temperature encountered in the cosmos, the cosmic microwave background temperature, a near-perfect black-body. The upper limit is so high that the most elements will be fully ionized so the properties of bound atomic states are not a concern.

Our density range extends from $N_e = 10^0 \text{ cm}^{-3}$, essentially the low-density limit, up to 10^{25} cm^{-3} , a density well above the lower regions of the atmospheres of accretion disks or stars. The partition function would normally be used in systems close to LTE, which requires higher densities (Hubeny & Mihalas 2014). Low-density gas is so far from equilibrium as to make many LTE concepts irrelevant (Osterbrock & Ferland 2006).

2.3. Definition of the partition function

The partition function is the sum over all quantum states of an atom with a degeneracy or statistical weight of g_n :

$$U = \sum_{n=1}^{\infty} g_n \exp\left(\frac{-E_n}{k_B T}\right) \quad (1)$$

where $\exp(-E_n/k_B T)$, the Boltzmann factor, gives the probability of the presence of an electron in some particular state, n , at temperature T , which has the energy of E_n . For a hydrogenic system, the statistical weight is

$$g_n = 2n^2 \quad (2)$$

The energy of the n -th shell for a hydrogenic atom, governed by the static screened Coulomb potential approximation, is

$$E_n = Z^2 I_H \left(1 - \frac{1}{n^2}\right) \quad (3)$$

where I_H is the ionization energy of the hydrogen atom, $I_H = 2.17 \times 10^{-11}$ erg.

For reference throughout this tutorial, Figure 1 shows energy levels of different species with an increasing number of orbiting electrons going from left to right. The level energies are given relative to the ionization energy, the red band at $y = 1$. Simple systems like H I have energy levels given by Equation 3, and have a simple structure. Complex systems have a far higher density of lower-energy states due to the complex interactions between various orbiting electrons. There is an infinite number of levels for all systems since n can, in theory, extend to infinity.

2.4. Ionization and excitation - the Boltzmann and Saha equations

The partition function plays a pivotal role in computing the LTE ionization and level excitation using the Saha and Boltzmann equations. The LTE ionization of atoms is given by the Saha equation, which, for the case of the hydrogen atom, is

$$\frac{N(\text{H II})}{N(\text{H I})} = \frac{2}{N_e} \left(\frac{2\pi m_e k_B T}{h^2}\right)^{\frac{3}{2}} \frac{U(\text{H II})}{U(\text{H I})} \exp\left(\frac{-I_H}{k_B T}\right) \quad (4)$$

where $U(\text{H I})$ and $U(\text{H II})$ represent the partition function for H I and H II. The Boltzmann constant, electron mass, Planck constant, and temperature are represented by k_B , m_e , h , and T , respectively. N_e

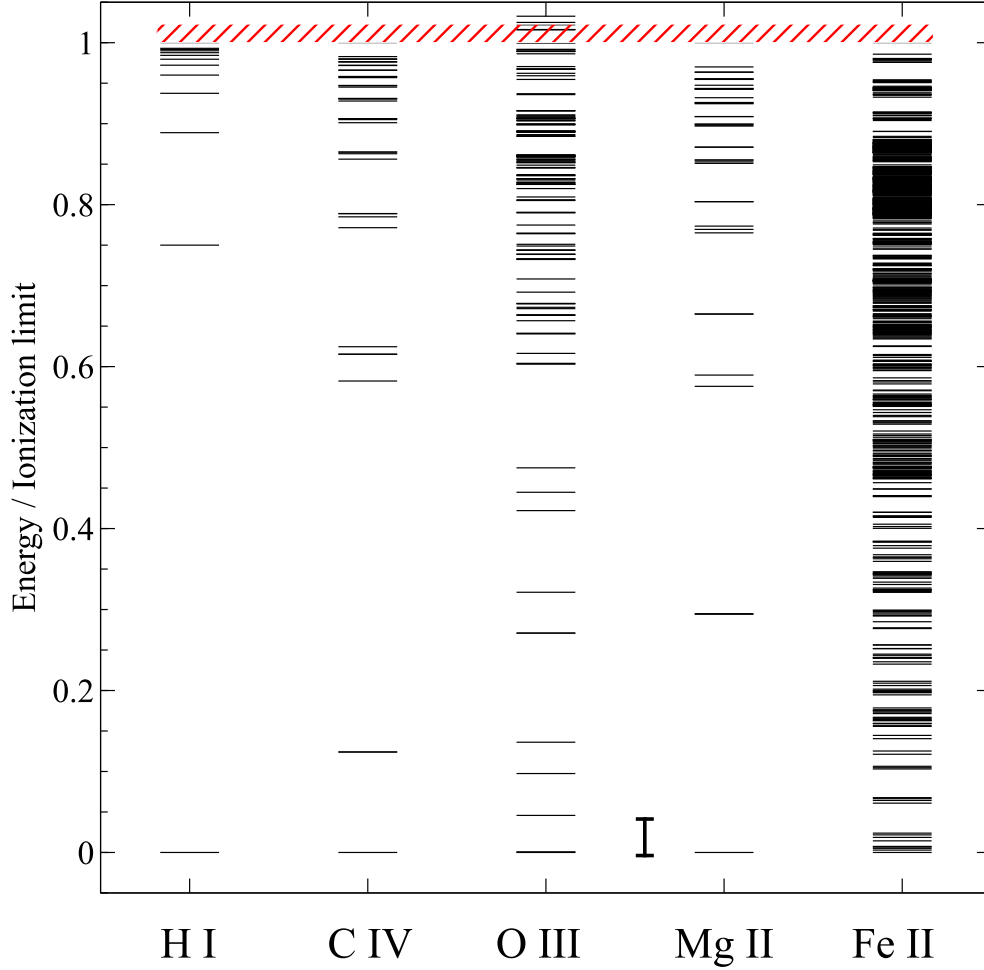


Figure 1. Experimental energy levels relative to each elements' ionization potential for some species presented in (Kramida et al. 2014) and adapted from Ferland et al. (2017). The red hashed lines show the scaled ionization limit. Those lines above the ionization limit shown for O III are auto-ionizing levels. As it is shown, for hydrogenic ions, most 1st and 2nd excited states are close to the continuum compared to the many-electron ions, where they are close to the ground state. The vertical line between O III and Mg II indicates an energy corresponding to $\sim 10^4$ K.

is the electron density [cm^{-3}]. Considering only atoms and ions, the conservation equation becomes

$$N(\text{H}) = N(\text{H I}) + N(\text{H II}) \quad (5)$$

allowing us to compute the ionization fractions of H I and H II relative to the total hydrogen density, $N(\text{H})$.

The Boltzmann equation gives the LTE level populations of atoms in a given excited state at some temperature. The population of the n -th shell will be

$$\frac{N_n(\text{H I})}{N(\text{H I})} = \frac{g_n}{U(\text{H I})} \exp\left(\frac{-E_n}{k_B T}\right) \quad (6)$$

where E_n is obtained by Equation 3. As shown in Equations 4 and 6, the partition function is required for the ionization and excitation calculations. The partition function of H II, a bare proton, is $U(\text{H II}) = 1$, a proton's statistical weight.

2.5. *The partition function for an infinite and finite atom*

This section outlines the behavior of the partition function. It is organized as follows:

The upper limit of the summation in Equation 1 includes all possible states. First, we show that this partition function diverges, it goes to infinity, for all temperatures where there is an infinite number of states.

We then numerically evaluate the partition function across a wide temperature range for a large but finite number of levels. The partition function does not go to infinity but does become very large at high temperatures. At low temperatures it takes the value of the statistical weight of the ground state. The very large- n levels that cause the divergence have a nonphysically large radius, and cannot exist in practical circumstances. This introduces the concept of the truncation of the partition function, the physics setting the highest- n that actually occurs. This should be the upper limit of the summation in Equation 1. This limit to the highest principal quantum number is discussed in Section 3.

2.5.1. *The divergent partition function for an infinite level atom*

We first show that the partition function will diverge for any T if the number of levels goes to infinity. For large n , the excitation energy of H I given by Equation 3 becomes the ionization energy:

$$\lim_{n \rightarrow \infty} E_n = \lim_{n \rightarrow \infty} I_{\text{H}} \left(1 - \frac{1}{n^2}\right) \approx I_{\text{H}}. \quad (7)$$

At high- n and T , where the kinetic energy $k_B T$ is much greater than the ionization energy I_{H} , we have $k_B T \gg I_{\text{H}} \implies k_B T \gg E_n$. The Boltzmann factors are all nearly unity, $\exp(I_{\text{H}}/k_B T) \rightarrow 1$,

since the argument in the exponential goes to zero. Then, $U_n \approx 2n^2$, the statistical weight of the n configuration, and $U = \sum_1^\infty U_n \rightarrow \infty$.

At low temperatures the term in the exponent in Equation 1 is large and negative. The Boltzmann factor becomes small, though finite. Therefore, no matter the temperature, the terms contributing to the partition function given by Equation 1 become infinity

$$\lim_{n \rightarrow \infty} U_n \approx \lim_{n \rightarrow \infty} 2n^2 \exp(-I_H/k_B T) \implies \infty. \quad (8)$$

The partition function diverges for all temperatures if the sum over principal quantum number is extended to infinity.

2.5.2. *The partition function for a finite atom*

This section evaluates U for a large but finite number of levels. It shows that U does not go to infinity; instead, it takes large values dominated by the highest levels. This introduces the concept of the truncation of the partition function. Here, we consider the partition function of H I at low-density and a broad range of T for large but finite numbers of levels to evaluate U .

Figure 2 shows a numerical evaluation of $U(\text{H I})$ versus T for three limits to the highest- n to the summation in Equation 1. The partition function remains finite for all T . At low- T , the Boltzmann equation (given by Equation 6) suggests that nearly all the atom's population is in the ground state. So only $n = 1$ contributes to the sum in Equation 1. Consequently, the partition function goes to $U(\text{H I}) \approx 2$, the statistical weight of the ground state.

The Boltzmann factors are all near unity at high T , so U becomes the sum of $2n^2$. This converges onto a high but finite plateau. The Boltzmann equation suggests that the probability of populating excited states increases as temperature increases, and so physically, nearly all the atom's population is in the highest levels. Therefore, the sum of $2n^2$ is dominated by the largest n , which accounts for the value of the plateau.

The infinite- n model in the previous section helps explain some of the behaviors in Figure 2. The Figure shows that the lowest temperature where U increases above 2 depends on the limit to the number of levels. So, we can estimate that extending $n \rightarrow \infty$ will increase the height of the plateau

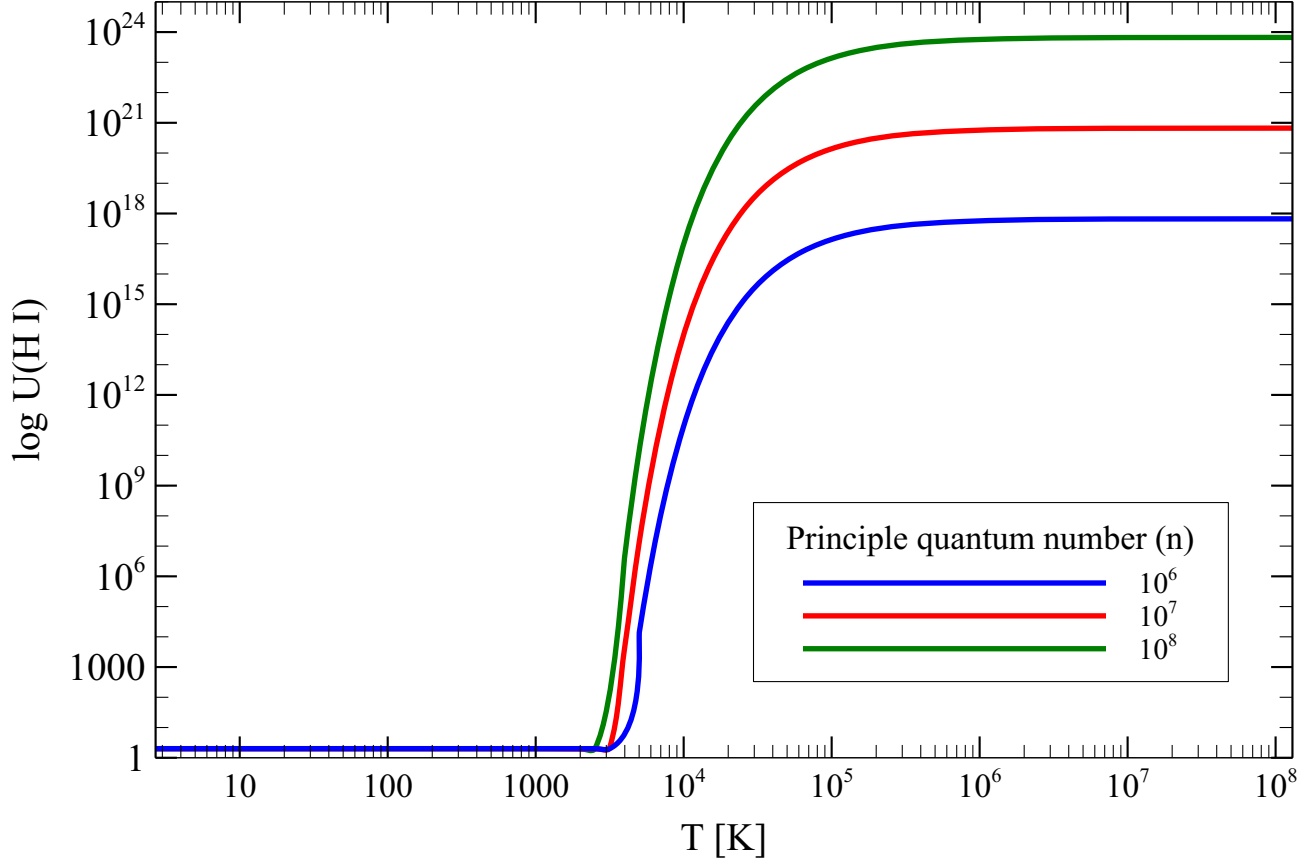


Figure 2. Partition Function versus limit to number of shells n and temperature. This shows $U(\text{H I})$ versus T for H I with the sum in Equation 1 extending to $n = 10^6$, 10^7 , and 10^8 . At low- T , the partition function is the statistical weight of the ground state, $g_n = 2$. U begins to increase when the temperature is high enough to populate the $n = 2$ configuration. At high temperatures, U is dominated by the highest n , which theoretically could go to infinity, demonstrating its divergent behavior.

at high- T and move the values in low- T to the left, and so $U(\text{H I})$ will go to infinity for the entire range of T .

Very large- n energy levels do not occur in nature because these orbits would have a nonphysically large radius. At low temperature, atoms mostly will be in the ground state, and an electron would have the most probable distance from the nucleus of one Bohr radius,

$$a_0 = \frac{4\pi\epsilon_0\hbar^2}{m_e e^2} = \frac{\hbar}{m_e c\alpha} \approx 5.29 \times 10^{-11} \text{ [m]} = 5.29 \times 10^{-9} \text{ [cm]} = 0.529 \text{ [\AA]} \quad (9)$$

where e is the elementary charge, and α is the fine structure constant, a dimensionless quantity independent of the system of units, and approximately is $\frac{1}{137}$.

At high temperatures, U is dominated by the highest n . The radius of an atom in the n^{th} shell of a hydrogenic ion with charge Z is

$$r = a_0 \left(\frac{n^2}{Z} \right) \approx 5.29 \times 10^{-11} \left(\frac{n^2}{Z} \right) [\text{m}] = 5.29 \times 10^{-9} \left(\frac{n^2}{Z} \right) [\text{cm}] = 0.529 \left(\frac{n^2}{Z} \right) [\text{\AA}]. \quad (10)$$

For a hydrogen atom with level numbers of $n = 10^6$, $n = 10^7$, and $n = 10^8$ that we discussed in Figure 2, Equation 10 gives radii of $r \approx 53$ [m], $r \approx 53 \times 10^2$ [m], and $r \approx 53 \times 10^4$ [m] respectively. These radii are far larger than the separations between hydrogen atoms at realistic densities. These orbits do not exist so U is finite.

Setting the upper limit to the sum giving n is the problem of establishing its truncation. The “hard sphere” model is the simplest approach for truncating the partition function. Here, the largest orbits are those that “fit” in the space between atoms. The following sections outline this, and more sophisticated, prescriptions for the truncation.

3. THE TRUNCATION OF THE PARTITION FUNCTION

The previous section reviewed the cause of the partition function’s divergence at higher temperatures. Current approaches for its truncation, as introduced in plasma or chemical references, are described here.

3.1. *Inter-particle interactions with Sharp cut-off*

In Section 2.5.2, we showed that for high temperatures, there are a large fraction of electrons in large orbits, which causes U given by Equation 1 to diverge. The physical problem is that the very large orbits cannot exist due to interactions with nearby atoms in a plasma. Taking these inter-particle interactions into account, one would set an upper limit for the number of states of an atom. The “hard sphere” model of the truncation is one example of how to do this. It can be visualized as the largest possible orbit that can fit between neutral and charged particles in a plasma.

The revised definition of the partition function is Halenka & Madej (2002)

$$U = \sum_{n=1}^{n_{\max}} g_n \exp \left(\frac{-E_n}{k_B T} \right) \quad (11)$$

In other words, interactions with neighboring particles in the plasma decrease the ionization potential I_{ion} by some amount of $\Delta\chi$, and so, the maximum energy of the largest bound orbit is

$$E_{\text{max}} = I_{\text{ion}} - \Delta\chi \quad (12)$$

where $\Delta\chi$ represents the lowering of the ionization energy, called “continuum lowering”. The goal is to find a theory that gives $\Delta\chi$ as a function of density or temperature. This type of theory gives a sharp cut-off to the divergence of the partition function.

There has been a tremendous effort to find a theory that gives a correct form of $\Delta\chi$ as a function of density and temperature. Some reviews of continuum-lowering theories due to Debye shielding, Stark, and collisional broadening have been developed especially within the plasma physics community and are described in [Inglis & Teller \(1939\)](#); [Unsöld \(1948\)](#); [Mihalas \(1978\)](#); [Hahn \(1997\)](#); [Milone & Merlo \(1998\)](#); [Bautista & Kallman \(2000\)](#); [Griem \(2005\)](#); [Capitelli et al. \(2012\)](#) or [Kallman et al. \(2020\)](#). These papers touch many different fields, ranging from laboratory plasmas to stars and astronomical plasma simulation codes like XSTAR ([Bautista & Kallman 2000](#)) or Cloudy ([Ferland et al. 2017](#)).

One example of these theories, Equation 9 – 106 in [Mihalas \(1978\)](#), gives a continuum-lowering criterion due to Debye shielding effect. The continuum is lowered by

$$\Delta\chi = 3 \times 10^{-8} Z N_e^{\frac{1}{2}} T^{-\frac{1}{2}} [\text{eV}], \quad (13)$$

a function of temperature, T , ionic charge, Z , and electron density, N_e .

We consider the case of H I ($Z = 1$) with sufficient lowering to decrease the ionization potential by $\Delta\chi = 1$ eV, to include only the first 4 configurations, where $n_{\text{max}} = 4$ is obtained using Equation 3. At $T = 2 \times 10^4$ K, Equation 13 gives the density of $N_e = 2.2 \times 10^{19} \text{ cm}^{-3}$.

Different theories predict that $\Delta\chi$ would have different density- and temperature- dependencies and results. Equations of 3, 4, and 5 of [Bautista & Kallman \(2000\)](#) and again in [Kallman et al. \(2020\)](#), (from [Inglis & Teller \(1939\)](#); [Hahn \(1997\)](#)) compare the continuum-lowering criteria for particle packing, Debye shielding, and Stark broadening. For $\Delta\chi = 1$ eV, particle packing finds a density of $N_e = 1.64 \times 10^{21} \text{ cm}^{-3}$, Debye shielding gives the density of $N_e = 3.57 \times 10^{31} \text{ cm}^{-3}$, and the Stark broadening gives the density of $N_e = 5.54 \times 10^{21} \text{ cm}^{-3}$. *These differ by 10 dex.* [Milone &](#)

Merlo (1998) presents the continuum lowering criterion with the nearest neighbor approximation (from Unsöld (1948)), which gives a density of $N_e = 2.91 \times 10^{18} \text{ cm}^{-3}$, *three dex below the lowest of the above*. The Debye shielding theory in Capitelli et al. (2012), their equation 8.4, gives a density of $N_e = 1.32 \times 10^{20} \text{ cm}^{-3}$. Including Debye shielding, the theories scatter over 14 dex in density. Excluding Debye shielding, the remaining theories scatter over ~ 3.5 dex. The reason for these divergent predictions is the difficulty in accurately describing the many-body interactions in a dense gas with a simple physical theory.

3.2. Inter-particle interactions with smooth cut-off

The inter-particle interactions discussed above sets an upper limit to the radius of an atom, solving the divergence of the partition function. However, the solution is not complete because interactions with neighboring ions perturb the electrons in lower orbits such that they become less bound to the nucleus. The probability that an orbit is filled so fully contributes to the partition function decreases as the distance from the nucleus increases. This revises the definition of the partition function to read Hummer & Mihalas (1988)

$$U = \sum_{n=1}^{n_{\max}} W_n g_n \exp\left(\frac{-E_n}{k_B T}\right) \quad (14)$$

The occupation probability, W_n , is the probability that an electron can be in the n -th orbit due to density effects. The numerical values of W_n start from 1 for fully occupied unperturbed levels and gradually decrease for the higher energy states and finally it goes to zero, $\lim_{n \rightarrow \infty} W_n = 0$ for large orbits that cannot exist. Some references, notably de Jager & Neven (1960), refer to W_n as the perturbation function while Hummer & Mihalas (1988), the most highly cited paper in this field, calls it the occupation probability.

A detailed study of the inter-particle interactions is required to determine the occupation probability. There are two types of interactions between particles within a plasma. The first determines the largest orbit for an atom by taking the separation between atoms into account and assuming the other interacting particles are in the ground state. The largest radius is related to the separation between particles. This is known as the *hard-sphere model* where the interactions are defined between

neutral particles and is describe in [Hubeny & Mihalas \(2014\)](#) and [Hummer & Mihalas \(1988\)](#). A numerical illustration of the hard-sphere model is presented in figure 8.14 of [Capitelli et al. \(2012\)](#).

The second model considers the electric field of these particles. That perturbs the higher atomic energy levels and leads to their depopulation. To know the details of these perturbations, one needs to obtain the electric field distribution of the charged particles in a plasma. The Holtsmark distribution function is a convenient way to describe interactions between all charged particles ([Hummer 1986](#)). However, it does not consider the motion of the particles, which means that it neglects the perturbations due to the magnetic field of the charged particles. As shown recently by [Vera Rueda & Rohrmann \(2020\)](#), the magnetic field of the charged perturbers disturb the higher energy levels as well.

Two theories describe W_n based on the inter-particle interactions, the *perturbation function model* ([de Jager & Neven 1960](#)), and the *occupation probability formalism* ([Hummer & Mihalas 1988](#)). The perturbation function model was developed to explain the gradual dissolution of the Lyman lines of the hydrogen atom as an analogy to the gradual depopulation of the higher energy levels due to their perturbations by ionized or neutral particles. Here, higher- n lines become indistinct and eventually disappear with the highest n depending on the density of the star's atmosphere. For more details see [de Jager & Neven \(1960\)](#).

The occupation probability model ([Hummer & Mihalas 1988](#)) describes the dissolution of the higher energy levels with the Stark effect and is by far the most widely used approach in stellar atmospheres. The occupation probability function takes the form

$$W_n = \int_0^{\beta_n} d\beta P_{\text{H}}(\beta) \quad (15)$$

where $P_{\text{H}}(\beta)$ is the Holtsmark function ([Hummer 1986](#)) and β_n is the reduced field strength. The final form of the occupation probability for both neutral and charged perturbers is given by Equation 4.71 of [Hummer & Mihalas \(1988\)](#). Their equation 4.42 gives the maximum level-number for a hydrogen-like system, with $W_{n_{\text{max}}} = e^{-1}$ and $\beta = 1.8$, by

$$n_{\text{max}} = 1.2 \times 10^3 N_e^{-2/15} Z_a^{3/5} \quad (16)$$

where Z_a is the ionic charge of the perturbers, and N_e is the number density of electrons. For more detail, we refer to [Hummer & Mihalas \(1988\)](#).

The next section considers U for H I but takes into account the ionization determined by the Saha equation. The ionization establishes an upper limit to the temperature where an ion has a significant abundance, providing another solution to the divergence of U at high temperatures.

4. ONE AND TWO-ELECTRON SYSTEMS; A SIMPLE LIMIT

We show next that the electronic structure of hydrogenic systems, together with the Saha equation, provide a simple solution to the divergence of U - namely, the partition function of 1 & 2 electron systems is well-behaved for temperatures where an ion has a large abundance.

4.1. *Asymptotic model with the Saha equation*

We use Equation 14 to compute $U(\text{H I})$ with the upper limit of the summation given by Equation 16 where ($Z_a = 1$). Since $W_n = 1$ is used for all energy levels, this is sometimes called the “*asymptotic version*” of the revised partition function. Figure 3 shows the LTE ionization fraction for H I and H II for a broad range of densities and temperatures. Figures 3a and 3c in linear and logarithmic scales respectively give results for the *ionic* ionization fractions. Figures 3b and 3d in linear and logarithmic scales respectively give the *atomic* ionization fractions.

These figures establish the temperature range where H I is abundant, and $U(\text{H I})$ matters. The highest practical temperature is the value where a significant amount of H I is still present. To set an upper limit to the temperature range, we use $\text{H I} / \text{H} \leq 0.001$, based on our Saha equation calculations. This limit could extend to $\text{H I} / \text{H} \leq 10^{-5}$ without any significant changes in the established temperature ranges. For these calculations, numerical values of $U(\text{H II}) = 1$ and $U(\text{H I}) = 2$ were used in Equation 4.

Figure 3 demonstrates that for lower electron densities, the hydrogen atom becomes ionized at quite low temperatures. As the electron density increases, the temperature needed to fully ionize hydrogen rises. The lower limit to the y-axis of Figures 3c and 3d is set to 10^{-3} to focus attention on the temperature range where H I is abundant. At these temperatures, H II becomes abundant, which is

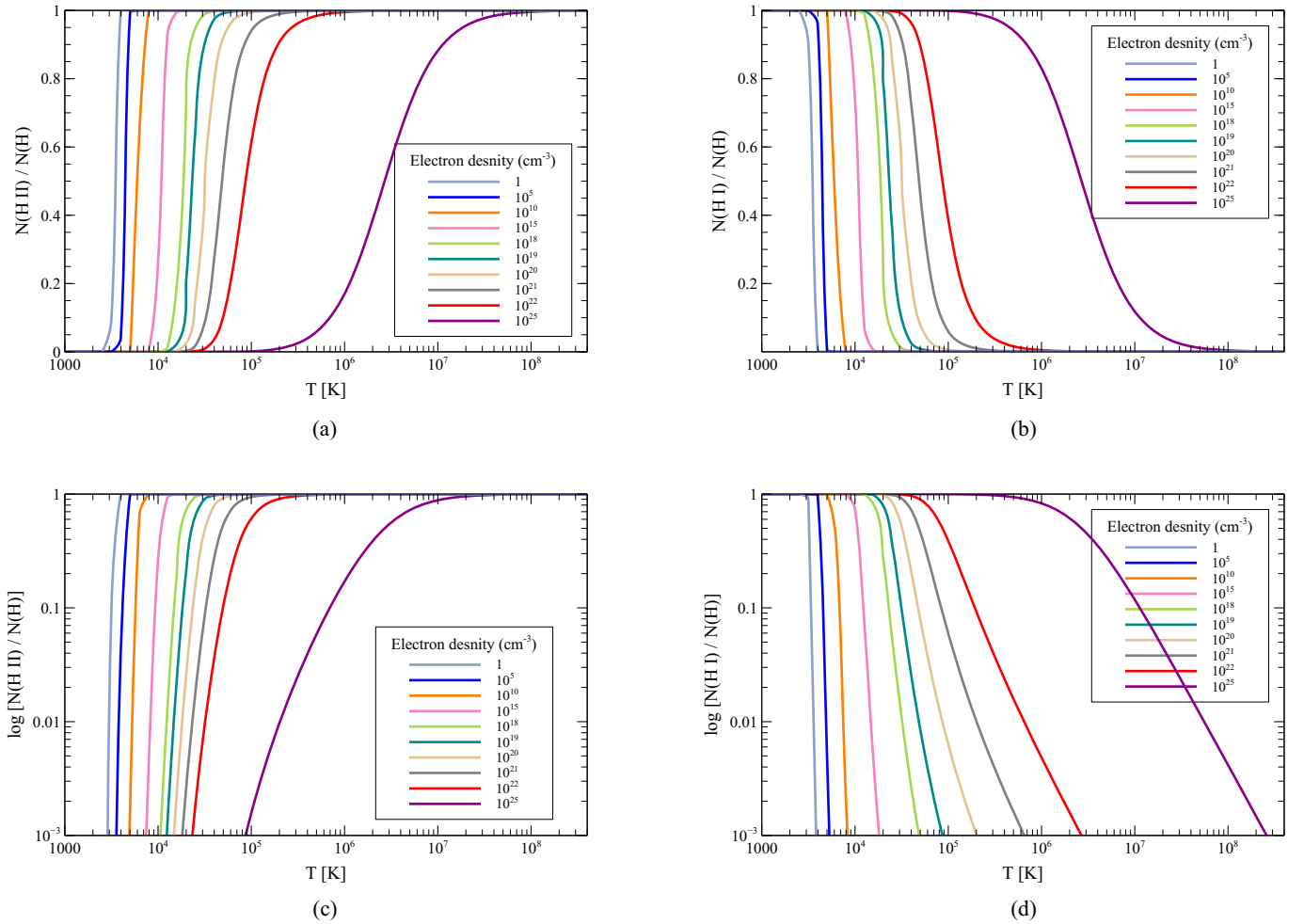


Figure 3. Saha Ionization Balance. (a): H II fraction in linear scale, (b): H I fraction in linear scale, (c): H II fraction in logarithmic scale, (d): H I fraction in logarithmic scale.

shown in Figures 3a and 3c. We also compute the correct H I partition function using Equation 16 as represented with the thin lines in Figure 4, which we will discuss later to derive an improved Saha ionization distribution. There is only a slight deviation between these Saha calculations for the range of electron densities from 10^{18} cm^{-3} to 10^{21} cm^{-3} due to using the uncertain truncation criterion for computing the partition function by Equation 16 or setting $W_n = 1$. However, for most densities and temperatures, this does not change our results.

In the next section, we evaluate $U(\text{H I})$ versus temperature limits obtained by the Saha equation and show that $U(\text{H I})$ does not diverge for most practical circumstances.

4.2. A practical upper limit to the temperature

Figure 4 shows U over the same range of temperatures and electron densities considered in Figure 3.

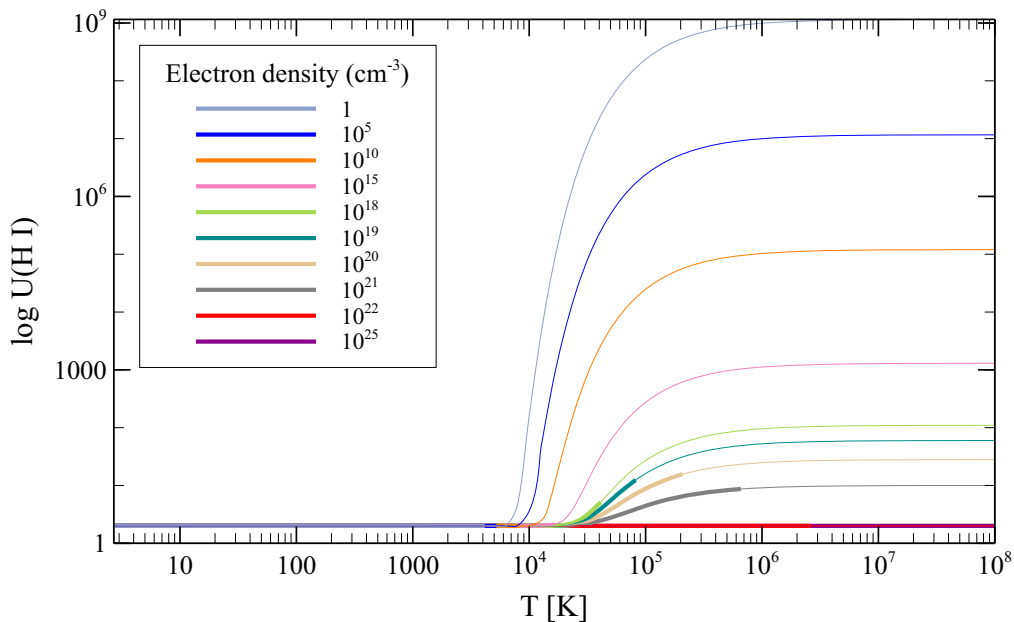
The thin lines in Figure 4 show $U(\text{H I})$ across for the full range. These lines deviate from the ground state statistical weight, 2, at moderate temperatures for the lower electron densities. The thick lines show U over the temperature range where H I is abundant. The temperature limits established in Section 4.1 were used to assess this. Figure 4 shows that for most densities and temperatures where H I is abundant, so the results are given by thick lines, $U \approx 2$. Only for a narrow range of densities, $10^{18} \text{ cm}^{-3} - 10^{21} \text{ cm}^{-3}$, is there a range of temperature where U is larger than 2. But, even in this range, U is not very large, $U(\text{H I}) \leq 10$.

Figure 4b expands the vertical axis to make this clearer. For very high densities like 10^{22} cm^{-3} or larger, $U(\text{H I})$ does not deviate from the ground state statistical weight for the entire range of temperatures because of the extreme lowering of the highest levels given by Equation 16.

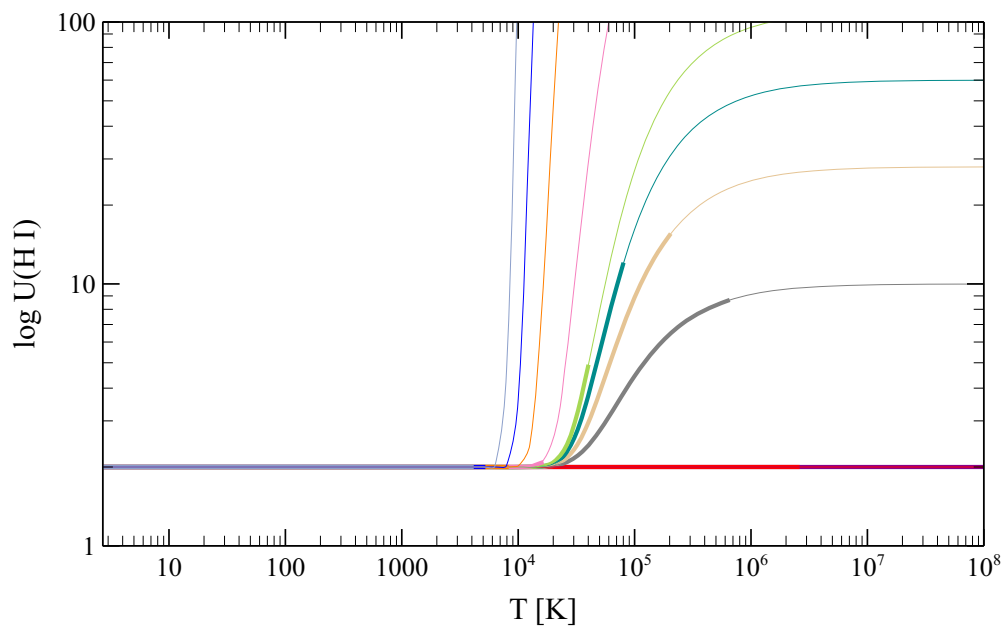
We provide another interpretation for $U(\text{H I})$ in Figure 4 using the energy levels of H I presented in Figure 1. Figure 1 shows that the lowest excited states of H I are closer to the continuum than the ground state. This means an electron in the third excited state, $n = 4$, has an energy $E_n \approx (1 - \frac{1}{n^2}) \approx 0.95$ of its ionization limit. At low temperatures, it does not contribute to U since its Boltzmann factor is small. When the gas is hot enough to populate $n = 4$, it is also hot enough to collisionally ionize the atom.

In general, the energy structure of hydrogenic systems means that most excited states are closer to the continuum than to the ground state, so if the population of the highly excited states is likely, then collisional ionization is too and the abundance is small. When the abundance of the atom is large, the highly excited states make a negligible contribution to the partition function.

Our results for 1 & 2 electron systems will tend to hold for any species with a closed-shell electronic structure due to the similar energy structure. For example, the one-electron systems: H I, He II, and Li III with $1s$ configuration, two-electron systems: He I, Li II, Be III, B IV, and C V with $1s^2$ configuration, and species with one electron in the L or M shell: Ne I, Na II, and Mg III with $1s^2 2s^2 2p^6$ configuration are closed-shell and roughly behave as quasi-hydrogenic species with a similar



(a)



(b)

Figure 4. The partition function of atomic hydrogen. The thin lines represent $U(\text{H I})$ for the full temperature range. The thick lines indicate the temperature range where $\text{H I} / \text{H} \geq 10^{-3}$. H is ionized to form H II at higher temperatures. Although the eye is drawn to the thin lines, for most temperatures and densities $U \sim 2$ and only rarely does it exceed 10.

explanation for the truncation of their partition function. Hence, the ground state approximation is an appropriate approximation for the partition function of the hydrogenic systems, or any system with a similar energy structure like closed-shell elements, and so $U(\text{H I}) \approx 2$ for most practical conditions.

This result explains the statements in some older texts (Novotny 1973; Swihart 1968) attributed to unpublished calculations of the Arthur. N. Cox, the author of Cox (2000). They note that the partition function of these species does not depend on temperature and density if the ions are abundant.

5. COMPLEX IONS - HERE BE DRAGONS

We have shown that the truncation of the partition function is uncertain. Considerable simplifications can be made in hydrogenic cases, although $U(\text{H I})$, does increase for low densities and high temperatures.

The situation is not so simple for many-electron systems. The energy levels associated with these ions are more complex, as shown in Figure 1. Fe II is a well-studied system that is observed in many astronomical sources. It has a complex energy structure, and here we consider it in detail.

Figure 5 shows $U(\text{Fe II})$ as a function of temperature, including all energy levels in Smyth et al. (2019) and used by Sarkar et al. (2021) in their study of high redshift quasars. There is no cut-off criterion and we assume $W_n = 1$. The highest temperature plotted is that at which Fe is collisionally ionized to form Fe III. To limit the temperature range, we used the condition $\text{Fe II} / \text{Fe} \leq 0.01$ and the ionization distribution represented in Nikolić et al. (2013). According to Figure 5, the partition function for Fe II is not severely divergent at the highest temperatures shown. Its evaluation is not as simple as 1 & 2 electron systems because it depends on the temperature across the entire range.

Figure 6 shows how $U(\text{Fe II})$ depends on the number of levels in Equation 11. This sum includes all states up to the energy index EI shown as the x-axis. $U(\text{Fe II})$ is evaluated at $T = 3 \times 10^4$ K since this is the most extreme case with the largest U . Continuum lowering limits EI so Figure 6 illustrates how U depends on density, assuming a density and temperature can be converted into EI .

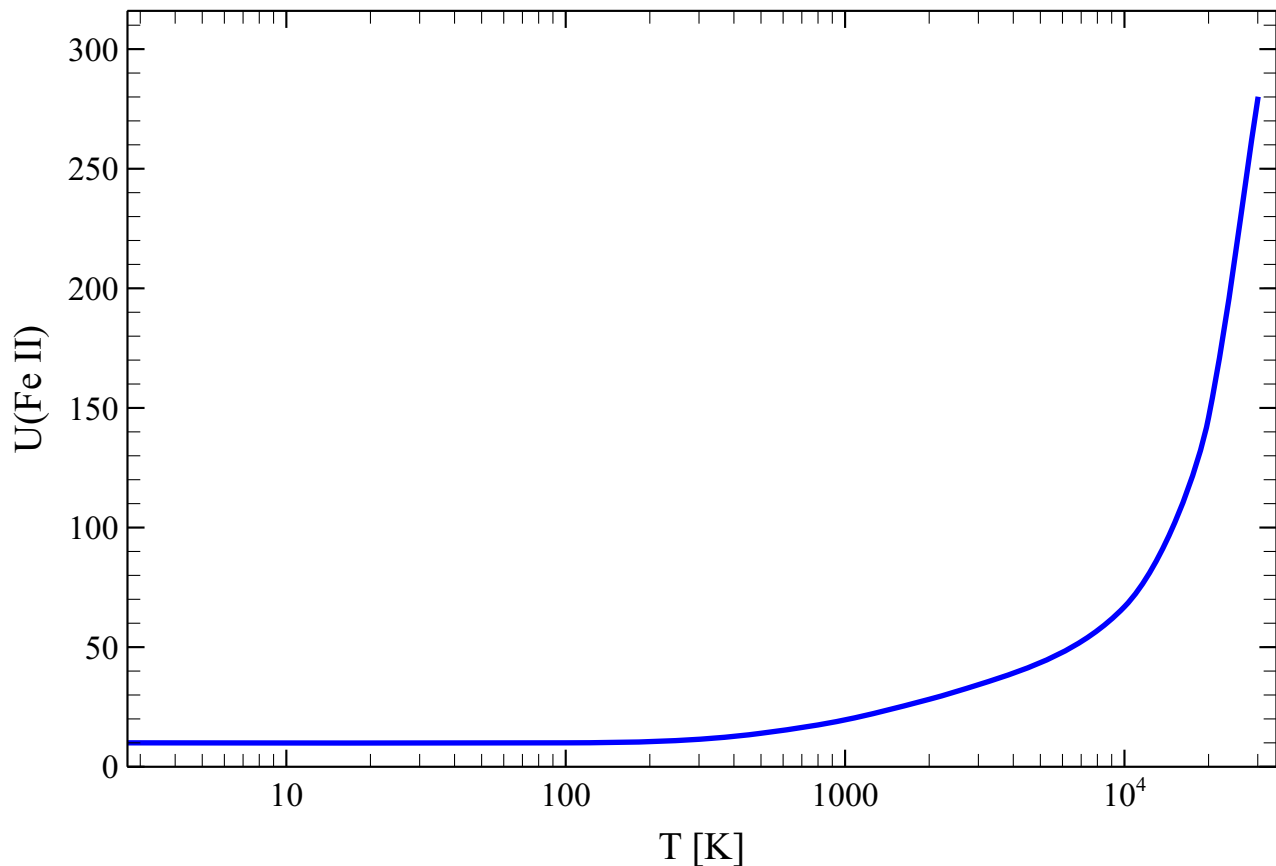


Figure 5. The partition function of Fe II. $U(\text{Fe II})$ is evaluated, including all energy levels presented in [Smyth et al. \(2019\)](#), over the temperatures where the Fe II abundance is significant. The high-temperature limit is where $\text{Fe II} / \text{Fe} \leq 0.01$ since Fe II is collisionally ionized to form Fe III.

The partition function sum has not fully converged since it is still increasing at the highest energy index. This suggests that highly excited and auto-ionizing energy levels present in the real atom but not in the [Smyth et al. \(2019\)](#) calculation might increase U farther. Figure 1 shows that many data sets have a gap between the highest listed level and the continuum above. There are actually an infinite number of very highly-excited levels in this gap. Sophisticated models of U , for instance [Halenka & Madej \(2002\)](#); [Halenka et al. \(2001\)](#), use atomic theory to account for these high levels and fill in this gap.

Extensive calculations of U for a wide variety of ions have been done. These often combine accurate experimental energy levels and use atomic theory to account for missing levels. Some examples include

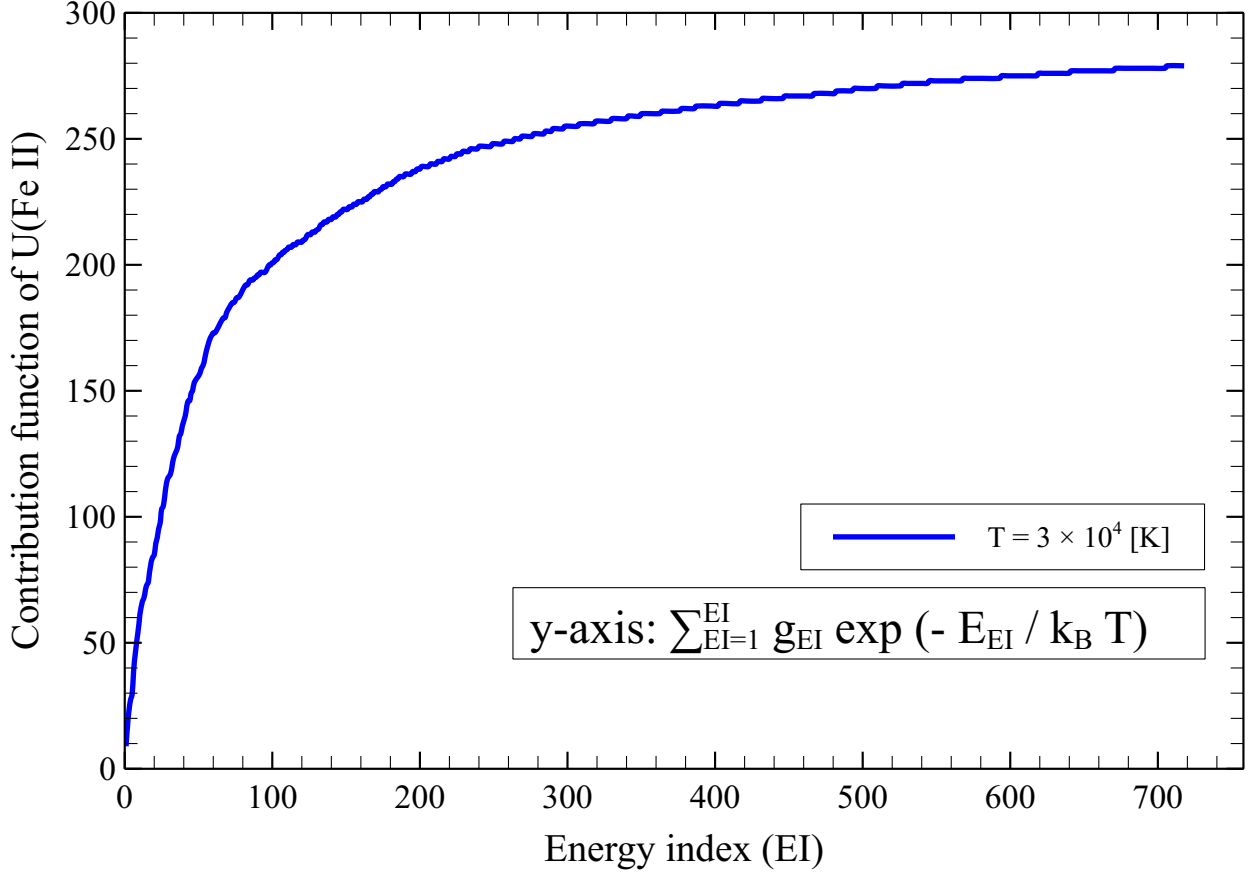


Figure 6. U for Fe II as a function of the number of levels included in the summation. It is evaluated for $U(\text{Fe II})$ at $T = 3 \times 10^4$ K. The number of levels included in Equation 11 is shown on the x-axis. Continuum lowering at high densities decreases the number of levels.

Milone & Merlo (1998) for H to Na, Halenka & Grabowski (1984) for Fe and Halenka et al. (2001) for Ni. Many papers present the equivalent of Figure 6 with the relationship between continuum truncation and density/temperature left as a separate problem. Table 1 lists examples.

There is no uncertainty in evaluating U as a function of the energy index in Figure 6. To find the highest energy index to include in the $U(\text{Fe II})$ sum, we need a truncation theory to map this index to the density and temperature effects in the dense plasma. Therefore, the next step is to evaluate $U(\text{Fe II})$ for realistic densities, which is equivalent to understanding the energy index in Figure 6 where W_n becomes small.

Table 1. Partition functions for complex ions

| Elements | reference |
|----------|-----------|
| H to Na | 1 |
| Ti, V | 2 |
| Cr | 3 |
| Fe | 4 |
| Mn, Co | 5 |
| Ni | 6 |

NOTE—References; 1 Milone & Merlo (1998) , 2 Halenka (1988), 3 Halenka & Grabowski (1986) , 4 Halenka & Grabowski (1984) , 5 Halenka (1989), 6 Halenka et al. (2001)

The challenge is to convert a particular density and temperature into the occupation probability or n_{\max} . Here, we consider the case of Fe II at $T = 3 \times 10^4$ K and a continuum lowering 4.6 eV. $\Delta\chi = 4.6$ eV below the ionization limit corresponds to energy index of $EI = 400$ in Figure 6. This is a maximum quantum number of $n_{\max} \approx 49$ in Equation 14 using the hydrogenic approximation. Equation 13 gives a required density of $N_e \approx 1.74 \times 10^{20}$ cm⁻³ to lower the continuum by this amount. One should be careful in applying the hydrogenic criterion to many-electron ions since the energy levels of the hydrogen-like species are explicitly related to the principal quantum number while this is not the case for many-electron ions unless we assume the hydrogenic energy level structure for these ions as well.

We discussed in Section 3.1, the continuum-lowering theories presented by Milone & Merlo (1998); Bautista & Kallman (2000); Capitelli et al. (2012) give different equations with different density dependencies. Equations 3, 4, and 5 in Bautista & Kallman (2000) give the densities of $N_e = 8.55 \times 10^{18}$ cm⁻³, $N_e = 6.09 \times 10^{29}$ cm⁻³, $N_e = 2.44 \times 10^{15}$ cm⁻³, respectively. More recently, Kallman et al. (2020) give a similar review of these equations. Milone & Merlo (1998) gives a density of $N_e = 7.09 \times 10^{19}$ cm⁻³. Equation 8.4 presented in Capitelli et al. (2012) gives the density of $N_e = 5.2 \times 10^{13}$ cm⁻³. And finally, Equation 16 for $n_{\max} = 49$ gives the density of $N_e = 5.12 \times 10^{11}$ cm⁻³. These theories are uncertain for the case of Fe II, as shown by the large discrepancies in the required densities, and this, in turn, is due to fundamental questions about plasma effects (Griem 2005).

Our case study of Fe II shows that while it is simple to specify the partition function as a number of levels, converting a particular density and temperature into a limit on the number of levels is uncertain. Extensive studies have been done showing U for most astrophysically abundant elements as a function of temperature and the highest level, or the degree of continuum lowering. We highlight two representative studies that evaluate U versus continuum lowering with no density dependency. [Halenka & Madej \(2002\)](#) studied Fe IV, (their figure 1 and table 1) for the temperature range where it is abundant. They include the higher energy levels missing from experiment but predicted by quantum mechanics, including auto-ionizing energy levels. They show how $U(\text{Fe IV})$ varies with continuum-lowering energy and temperature. The same evaluation for Ni IV is shown in figure 1 presented in [Halenka et al. \(2001\)](#).

[D’Ammando et al. \(2013\)](#) shows another example using the pressure-lowering criterion. They evaluate the partition function for carbon, C I - C IV, using the three so-called lumped levels of the ground state, low-lying excited states called 1st excited states, and the rest called 2nd excited states. The result is shown in figure 1 of the paper. Like the partition function of Fe IV, the partition function is evaluated versus temperature and continuum lowering. These authors do not attempt to convert a temperature or density into the explicit continuum lowering that will occur. That last step is the essential difficulty with only discrepant theories available to the worker.

These issues are also present in laboratory plasmas like Tokamaks ([Ralchenko 2016](#)). Here, spectra are used to probe conditions in the plasma, so getting the “right answer” is important. The dense-plasma community organizes a series of “NLTE” workshops, which gather developers of spectral simulation codes to compare results and discuss physical methods. We have participated in two of these workshops, summarized by [Chung et al. \(2013\)](#) and [Piron et al. \(2017\)](#), and presented predictions of the spectral synthesis code Cloudy ([Ferland et al. 2017](#)). [Kallman et al. \(2020\)](#) include predictions of XSTAR ([Bautista & Kallman 2000](#)) in another workshop. The plasma codes are not in good agreement at high densities due to various treatments of collisional effects upon highly excited states. These and other dense-plasma challenges are reviewed by [Ralchenko \(2016\)](#).

6. THE MOLECULAR PARTITION FUNCTION

We do not discuss the molecular partition function, but we could extend our results based on the energy structure to examine this behavior. Molecules have a very different energy-level structure, making their properties very different from what we have described for simple or complex ions. The essential difference is that molecules do not have an infinite number of rotational-vibrational levels. The rotational energy-level spacing increases as the energy increases, so there are only a few highly excited states. This property of the energy structure of molecules is shown in figures 2 and 3 presented in [Shaw et al. \(2005\)](#) for H_2 , which can be compared with Figure 1. The divergence and truncation of the molecular partition function is not a central concern for these low levels. For further discussions about the molecular partition function, the reviews by [Sauval & Tatum \(1984\)](#); [Mangum & Shirley \(2015\)](#) are useful. Polynomial expansions for diatomic molecules of astrophysical interest are given by [Sauval & Tatum \(1984\)](#).

7. DISCUSSION, SUMMARY, AND CONCLUSION

This tutorial offers an introduction to numerical calculations of the partition function U . Accurate values are needed to predict the populations or ionization of a gas in thermodynamic equilibrium or local thermodynamic equilibrium. Although texts do cover the definition of U , and some give it as the statistical weight of the ground state, we know of none which provide practical advice on obtaining numerical values for U for a particular density and temperature.

Our major points are:

- The partition is infinite for any atom with an infinite number of levels. This is referred to as the divergence of the partition function. Although the principal quantum number n can extend to infinity in quantum mechanics, the radius of the orbit also goes to infinity. Large orbits are not possible since an atom would overlap with its neighbors. There must be the largest possible orbit that would be smaller for a denser gas. This introduces the concept of a density-dependent cutoff or truncation to the number of levels included in Equation 1. This is often referred to as continuum lowering at high densities.

- Calculating U is relatively simple for one and two electron atoms like hydrogen or helium, because their orbits have the hydrogenic spacing shown in Figure 1. The larger orbits which cause U to diverge are very close to the continuum. Temperatures high enough to populate the highest levels would also ionize the atom so there is an upper limit to the temperature where the atom is abundant and U matters. By combining the Saha and Boltzmann equations we show that for most conditions U is the statistical weight of the ground state. It increases to modest values, generally $U < 10$, for a narrow range of density and temperature.
- The energy-level structure of many-electron systems like Fe II, also shown in Figure 1, is far more complex. We need a theory to specify how many levels to include in Equation 1. Figure 5 shows U for Fe II over a range of temperature while Figure 6 shows the effects of varying the number of levels, which is equivalent to varying the density since continuum lowering is more severe at high densities.
- Two approaches are taken to truncate the number of levels that contribute to U . The hard-sphere model establishes a largest level that can exist in the space available between atoms and ions. This sets an upper limit to the sum in Equation 1 as given in Equation 11. The occupation probability method assigns a likelihood W_n that a level is occupied. The sum becomes Equation 14. Both approaches are used.
- The stellar astrophysics community has adopted the approach of Hummer & Mihalas (1988), with over six hundred citations listed in the ADS. They describe the dissolution of the higher energy levels with the Stark effect. Other theories are used in other communities such as accretion flows near black holes (Kallman et al. 2020) or a laboratory plasma (Ralchenko 2016). The various theories differ by large amounts giving densities that can range over more than one dex for a given truncation. This shows the difficulty in treating the effects of the sea of free electrons that surround an atom in a dense gas. This is a long-standing and vexing problem that spans many parts of physics.

ACKNOWLEDGMENTS

GJF acknowledges support by NSF (1816537, 1910687), NASA (ATP 17-ATP17-0141, 19-ATP19-0188), and STScI (HST-AR- 15018).

REFERENCES

- Allen, C. W. 1973, *Astrophysical quantities*
- Bautista, M. A., & Kallman, T. R. 2000, *ApJ*, 544, 581, doi: [10.1086/317206](https://doi.org/10.1086/317206)
- Blundell, S., & Blundell, K. 2010, *Concepts in Thermal Physics* (OUP Oxford). <https://books.google.com/books?id=T0luBAAAQBAJ>
- Bradt, H. 2014, *Astrophysics Processes*
- Capitelli, M., Colonna, G., & D'Angola, A. 2012, *Fundamental Aspects of Plasma Chemical Physics*, Vol. 66, doi: [10.1007/978-1-4419-8182-0](https://doi.org/10.1007/978-1-4419-8182-0)
- Carroll, B. W., & Ostlie, D. A. 2006, *An Introduction to Modern Astrophysics*
- Chung, H. K., Bowen, C., Fontes, C. J., Hansen, S. B., & Ralchenko, Y. 2013, *High Energy Density Physics*, 9, 645, doi: [10.1016/j.hedp.2013.06.001](https://doi.org/10.1016/j.hedp.2013.06.001)
- Cox, A. N. 2000, *Allen's astrophysical quantities*
- D'Ammando, G., Colonna, G., & Capitelli, M. 2013, *Physics of Plasmas*, 20, 032108, doi: [10.1063/1.4794286](https://doi.org/10.1063/1.4794286)
- de Galan, L., Smith, R., & Winefordner, J. D. 1968, *Spectrochimica Acta*, 23, 521, doi: [10.1016/0584-8547\(68\)80032-1](https://doi.org/10.1016/0584-8547(68)80032-1)
- de Jager, C., & Neven, L. 1960, *BAN*, 15, 55
- Ferland, G. J., Chatzikos, M., Guzmán, F., et al. 2017, *Revista Mexicana de Astronomía y Astrofísica*, 53, 385. <https://arxiv.org/abs/1705.10877>
- Griem, H. R. 2005, *Principles of Plasma Spectroscopy*
- Hahn, Y. 1997, *Physics Letters A*, 231, 82, doi: [10.1016/S0375-9601\(97\)00287-9](https://doi.org/10.1016/S0375-9601(97)00287-9)
- Halenka, J. 1988, *A&AS*, 75, 47
- . 1989, *A&AS*, 81, 303
- Halenka, J., & Grabowski, B. 1984, *A&AS*, 57, 43
- . 1986, *A&AS*, 64, 495
- Halenka, J., & Madej, J. 2002, *AcA*, 52, 195. <https://arxiv.org/abs/astro-ph/0204384>
- Halenka, J., Madej, J., Langer, K., & Mamok, A. 2001, *AcA*, 51, 347. <https://arxiv.org/abs/astro-ph/0201238>
- Hubeny, I., & Mihalas, D. 2014, *Theory of Stellar Atmospheres*
- Hummer, D. G. 1986, *JQSRT*, 36, 1, doi: [10.1016/0022-4073\(86\)90011-7](https://doi.org/10.1016/0022-4073(86)90011-7)
- Hummer, D. G., & Mihalas, D. 1988, *ApJ*, 331, 794, doi: [10.1086/166600](https://doi.org/10.1086/166600)
- Inglis, D. R., & Teller, E. 1939, *ApJ*, 90, 439, doi: [10.1086/144118](https://doi.org/10.1086/144118)

- Kallman, T., Bautista, M., Deprince, J., et al. 2020, arXiv e-prints, arXiv:2011.10603.
<https://arxiv.org/abs/2011.10603>
- Kramida, A., Ralchenko, Y., & Reader, J. 2014, in APS Division of Atomic, Molecular and Optical Physics Meeting Abstracts, APS Meeting Abstracts, D1.047
- Mangum, J. G., & Shirley, Y. L. 2015, PASP, 127, 266, doi: [10.1086/680323](https://doi.org/10.1086/680323)
- Mihalas, D. 1978, Stellar atmospheres
- Milone, L. A., & Merlo, D. C. 1998, Ap&SS, 259, 173, doi: [10.1023/A:1001508021614](https://doi.org/10.1023/A:1001508021614)
- Nikolić, D., Gorczyca, T. W., Korista, K. T., Ferland, G. J., & Badnell, N. R. 2013, ApJ, 768, 82, doi: [10.1088/0004-637X/768/1/82](https://doi.org/10.1088/0004-637X/768/1/82)
- Novotny, E. 1973, Introduction to stellar atmospheres and interiors
- Osterbrock, D. E., & Ferland, G. J. 2006, Astrophysics of gaseous nebulae and active galactic nuclei
- Piron, R., Gilleron, F., Aglitskiy, Y., et al. 2017, High Energy Density Physics, 23, 38, doi: [10.1016/j.hedp.2017.02.009](https://doi.org/10.1016/j.hedp.2017.02.009)
- Ralchenko, Y. 2016, Modern Methods in Collisional-Radiative Modeling of Plasmas
- Sarkar, A., Ferland, G. J., Chatzikos, M., et al. 2021, ApJ, 907, 12, doi: [10.3847/1538-4357/abcaa6](https://doi.org/10.3847/1538-4357/abcaa6)
- Sauval, A. J., & Tatum, J. B. 1984, ApJS, 56, 193, doi: [10.1086/190980](https://doi.org/10.1086/190980)
- Shaw, G., Ferland, G. J., Abel, N. P., Stancil, P. C., & van Hoof, P. A. M. 2005, ApJ, 624, 794, doi: [10.1086/429215](https://doi.org/10.1086/429215)
- Smyth, R. T., Ramsbottom, C. A., Keenan, F. P., Ferland, G. J., & Ballance, C. P. 2019, MNRAS, 483, 654, doi: [10.1093/mnras/sty3198](https://doi.org/10.1093/mnras/sty3198)
- Swihart, T. L. 1968, Astrophysics and stellar astronomy
- Unsöld, A. 1948, ZA, 24, 355
- Vera Rueda, M., & Rohrman, R. D. 2020, A&A, 635, A180, doi: [10.1051/0004-6361/201937413](https://doi.org/10.1051/0004-6361/201937413)